NEOPLASIA
www.neoplasia.com

Volume 13 Number 9 September 2011 pp. 841–853 841

# Hypomethylation of the hsa-miR-191 Locus Causes High Expression of hsa-miR-191 and Promotes the Epithelial-to-Mesenchymal Transition in Hepatocellular Carcinoma[1,2]

**Yinghua He*[,3], Ying Cui[†,3], Wei Wang*, Jun Gu*, Shicheng Guo*, Kelong Ma* and Xiaoying Luo***

*State Key Laboratory of Oncogenes and Related Genes, Renji Hospital, Shanghai Jiaotong University School of Medicine, Shanghai Cancer Institute, Shanghai, China; [†]Guangxi Cancer Institute, Nanning, Guangxi, China

## Abstract

hsa-miR-191 is highly expressed in hepatocellular carcinoma (HCC), but the factors regulating this elevated expression are unknown. This study aimed to investigate the epigenetic mechanisms of increased hsa-miR-191 expression by analyzing the relationship between the DNA methylation status of hsa-miR-191 and miR-191 expression. Methylation-specific polymerase chain reaction (PCR), bisulfite sequencing PCR, Northern blot, and quantitative real-time PCR were performed to examine hsa-miR-191 methylation and expression levels. Western blot, transwell, and scratch assays were performed to examine the function and molecular mechanisms of hsa-miR-191. Approximately 58.9% of hsa-miR-191 expression was higher in HCC tissues than in adjacent noncancerous tissues; this high expression was associated with poor prognosis. The hypomethylation observed in some HCC cell lines and HCC tissues was correlated with the hsa-miR-191 expression level. This correlation was validated by treatment with the 5-aza-DAC demethylation agent. The level of hypomethylation was 63.0% in 73 clinical HCC tissue samples and was associated with increased (2.1-fold) hsa-miR-191 expression. The elevated expression of hsa-miR-191 in the SMMC-771 HCC cell line induced the cells to transition into mesenchymal-like cells; they exhibited characteristics such as loss of adhesion, down-regulation of epithelial cell markers, up-regulation of mesenchymal cell markers, and increased cell migration and invasion. Inhibiting hsa-miR-191 expression in the SMMC-7721 cell line reversed this process (as assessed by cell morphology and cell markers). Furthermore, hsa-miR-191 probably exerted its function by directly targeting TIMP metallopeptidase inhibitor 3 and inhibiting TIMP3 protein expression. Our results suggest that hsa-miR-191 locus hypomethylation causes an increase in hsa-miR-191 expression in HCC clinical tissues and that this expression induces HCC cells to transition into mesenchymal-like cells.

*Neoplasia (2011) 13, 841–853*

## Introduction

Hepatocellular carcinoma (HCC) is one of the most common human malignancies worldwide, with a particularly high prevalence in East Asia and South Africa [1]. Although the risk factors for HCC, which include hepatitis B and C virus infections, aflatoxin B exposure, and heavy consumption of alcohol, are well documented, its molecular pathogenesis remains poorly understood. In the past two decades, there has been great progress in the identification of candidate HCC-related protein-coding genes. By contrast, little is known about the roles of functional noncoding sequences related to HCC, particularly those of microRNAs (miRNAs).

Address all correspondence to: Xiaoying Luo, PhD, Shanghai Cancer Institute, No. 25/Ln2200, XieTu Rd, Shanghai, 200032, China. E-mail: lxybio@gmail.com

[1]This work was supported by a Grant-in-Aid for Young Scientists Foundation of the Shanghai Cancer Institute (SB09-08) and the Natural Science Foundation of China (grant 30660203). There are no competing financial interests.
[2]This article refers to supplementary materials, which are designated by Tables W1 to W4 and Figure W1 and are available online at www.neoplasia.com.
[3]These authors contributed equally to this work.
Received 16 May 2011; Revised 30 June 2011; Accepted 1 July 2011

Copyright © 2011 Neoplasia Press, Inc. All rights reserved 1522-8002/11/$25.00
DOI 10.1593/neo.11698

DNA methylation is a type of epigenetic modification. Aberrant methylation, consisting of DNA hypomethylation and/or promoter gene CpG hypermethylation, is implicated in the development of a variety of solid tumors, including HCC [2]. Cirrhosis [3], chronic hepatitis [4], and alcohol consumption can induce liver lesions [4]. Aberrant DNA methylation is associated with liver lesions, which could induce HCC. Previous research that has focused on DNA methylation as a biomarker for the DNA methylome (microarray-based studies) has shown that there are differences in the levels of DNA methylation in various liver lesions (normal liver, hepatitis, cirrhosis, and HCC). Therefore, evaluation of the status of DNA methylation could aid in diagnosing, determining the prognosis of, and helping to predict the risk of carcinogenesis in HCC.

miRNAs are small, endogenous, noncoding RNAs that serve as posttranscriptional regulators of gene expression [5]; they bind to the 3′ untranslated regions (UTRs) of target mRNAs and either prevent their translation or cause their degradation. Accumulating evidence has shown that miRNAs have crucial functions in a number of cellular and biologic processes [6]. The deregulation of miRNAs plays an important role in a wide range of human diseases, including cancers [7]. Several studies have demonstrated that various miRNAs are deregulated in HCC tissue samples compared with noncancerous liver tissue controls. Other research has focused on identifying the factors that regulate the expression of miRNAs in hepatic carcinogenesis; for example, DNA methylation or transcription factors could regulate the expression of miR-1 [8] and miR-124/miR-203 [9]. The most well-studied topics in determining the molecular mechanism of miRNAs is research on cancer phenotype and miRNA targeting of genes. The factors that regulate miRNA expression are not clear; in particular, the role of DNA methylation, an epigenetic regulatory factor that controls miRNA transcription, has not been clarified.

In this study, we sought to identify miRNAs that are regulated by DNA methylation. We obtained a DNA methylome, miRNA profile, and mRNA profile in normal liver tissue and six HCC cell lines. We found a target miRNA, miR-191, and then validated the correlation of DNA methylation and expression for 73 pairs of clinical tissues from HCC patients.

## Materials and Methods

### *Human Tissues*

Human primary HCC and adjacent, noncancerous liver tissues (3 cm from the tumor) were collected from the surgical specimen archives of Guangxi Medical University, Guangxi Province, China. One of the two normal liver tissue samples was collected from a person who died because of an accident; the other was purchased from Clontech (Palo Alto, CA). All human materials were obtained with informed consent, and the institutional ethics review committee of the Shanghai Cancer Institute approved the protocols used in this study. Clinical information was collected from patients' records; details are listed in Table W4.

### *Cell Lines and 5-Aza-DAC Treatments*

SMMC-7721, QGY-7703, PLC/PRF/5, BEL-7402, HepG2, and Hep3B human HCC cancer cell lines were used. Cells were cultured in Dulbecco modified Eagle medium/F-12 (1:1) medium supplemented with 10% bovine calf serum (PAA Laboratories, Dartmouth, MA) and antibiotics (Gibco, Invitrogen, Carlsbad, CA). The hsa-miR-191–overexpressing SMMC-7721 cell line and its control were cultured on poly-L-lysine (0.1 mg/ml; Sigma-Aldrich, St Louis, MO)–precoated plates. The QGY-7402 cell line was seeded at a density of $10^6$ cells/10-cm dish, cultured for 48 hours, and treated with freshly prepared 5 μM 5-Aza-CdR (Sigma-Aldrich) dissolved in 50% acetic acid.

### *Transfections*

MicroRNA mimics and miRNA antagomiRs were designed and synthesized by RiboBio (Guangzhou China). The miRNA antagomiRs were all nucleotides with a 2′-*O*-methyl modification. The miRNA mimics were transiently transfected with Lipofectamine 2000 (Invitrogen) according to the manufacturer's protocol. The miRNA antagomiRs were transiently transfected with Amaxa Nucleofector (Amaxa, Koeln, Germany) according to the manufacturer's protocol.

### *DNA Preparation, RNA Extraction, and Quantitative Real-time Polymerase Chain Reaction*

Genomic DNA was isolated using the QIAamp DNA Mini Kit (Qiagen, Valencia, CA) according to the manufacturer's protocol. Total RNA was isolated using TRIzol Reagent for Molecular Biology (Invitrogen/Life Technologies). Genomic DNA from tumor samples was purified by standard phenol/chloroform purification. DNA quality was verified by electrophoresis through an agarose gel and visualized with ethidium bromide. For microarray experiments, total RNA was further purified using the RNeasy Mini Kit (Qiagen). For quantitative real-time polymerase chain reaction (qRT-PCR), 5 μg of total RNA was previously treated with the RQ1 RNase-free DNase (Promega, Madison, WI). The complementary DNA of genes was synthesized using the TIANScript RT Kit (Tiangen, Beijing, China). The complementary DNA from the miRNA was synthesized using the Quant Reverse Transcriptase (Tiangen) and an reverse transcript primer from RiboBio. Real-time PCR analyses were performed with Real MasterMix (SYBR Green; Tiangen) using synthesized primers that were purchased from RiboBio. The primers for the hsa-miR-191 host gene *DALRD3* and its antisense gene *NDUFAF3* were designed using the Web site http://pga.mgh.harvard.edu/primerbank/:

DALRD3RTF: 5′ AGGCTGACAGCAGTATCTCCAC 3′
DALRD3RTR: 5′ GAGCAACAACCACTCACCCTC 3′
NDUFAF3RTF: 5′ GACATCACCGAAGACAGCTTT 3′
NDUFAF3RTR: 5′ CACCACCACGATCTCTATCCG 3′

### *Bisulfite Treatment and Methylation-Specific and Bisulfite-Sequencing PCR Analyses*

The bisulfite conversion and PCR analyses were performed as described previously [10]. The primers involved in methylation-specific (MSP) and bisulfite-sequencing PCRs (BSP) were designed using the Web site (http://www.urogene.org/methprimer/index1.html). To design the primers, the target sequence from the region with a methylation signal in the DNA methylome was used, taking into consideration the repeat sequence around the target sequence. The following primers were used for the BSP assay: hsa-miR-191bspf, 5′ TGGTTGTTGTTTAAAATAGGAA 3′; and hsa-miR-191bspt, 5′ TACCTCAATCTCCCAAATAACT 3′. The following primers were used for the MSP assay: Msp forward methylation primer, 5′ TTTAAAATAGGAAGTTTTAAGGATCGT 3′; Msp reverse methylation primer, 5′ AAATAACTAAAATTACAAACACGCG 3′; Msp

forward nonmethylation primer, 5′ TTTAAAATAGGAAGTTTTAAGGATTGT 3′; and Msp reverse nonmethylation primer, 5′ ATAACTAAAATTACAAACACACACC 3′. The $T_m$ was 52°C, and there were 35 PCR cycles.

### *Vector Constructs*

A putative hsa-miR-191 binding site in the TIMP metallopeptidase inhibitor 3 (TIMP3) 3′UTR was inserted downstream of a cytomegalovirus promoter-driven firefly luciferase cassette in a pCDNA3.0 vector. The following oligos were used: TIMP3 Ecf, 5′ AATTGTTGCCTTAGGGTTTTCGTCGACT 3′; and TIMP3 Xbt, 5′ CTAGAGTCGACGAAAACCCTAAGGCAAC 3′. These oligos annealed and were ligated to the vector.

### *Lentiviral Production and Transduction*

Virus particles carrying the hsa-pri-miR-191 precursor and its control were purchased from GENECHEM (Shanghai, China). The lentiviral transduction was carried out according to advice from GENECHEM. The resulting cells were seeded onto 96-well plates and cultured for 2 months to produce a stable hsa-miR-191–overexpressing cell line. The high expression was validated by qRT-PCR.

### In Vitro *Migration and Invasion Assays*

The invasion assays were performed using the Neuro Probe Standard 12-well Chemotaxis Chamber (catalog no. AA12; Gaithersburg, MD). The lower wells were filled with complete culture medium, and the upper wells, which contained 5000 cells, were filled with medium lacking serum. The porous polycarbonate membrane (8-μm pores) separating the two wells was coated with Matrigel (BD Biosciences).

Migration assays were performed by seeding cells onto a six-well plate coated with fibronectin (Sigma-Aldrich). After the cells that were attached to the plate reached 100% confluence, the confluent monolayer was scratched using a sterile pipette tip. Photographs of cell migration into the scratched area were taken, and statistical analysis was performed on five randomly chosen fields.

### *Northern and Western Blots*

Northern blots were performed as reported previously [11]. The optimized hybridization temperature for the probe against hsa-miR-191 was 39°C. The following probes were used in the Northern blot assay: hsa-miR-191, 5′ CAGCTGCTTTTGGGATTCCGTTG 3′; and U6, 5′ AACGCTTCACGAATTTGCGT 3′. Twenty micrograms of total RNA was loaded into each well.

Proteins were separated by SDS-PAGE and transferred to a poly (vinylidene fluoride) membrane (Bio-Rad, Hercules, CA). The membrane was blocked with 5% nonfat milk and incubated with mouse anti–pan-cytokeratin monoclonal antibody (1:1000), antiactin monoclonal antibody (1:2000; Santa Cruz Biotechnology, Santa Cruz, CA), rabbit anti–E-cadherin (1:50), N-cadherin (1:50), TIMP3 (1:100), and vimentin (1:500) polyclonal antibodies (Abgent, Inc, San Diego, CA).

The resulting RNA and protein bands were quantified using ImageQuant Capture software (version 1.0.0; GE Healthcare Life Sciences, Piscataway, NJ).

### *DNA Methylome, miRNA, and mRNA Expression Profiles*

The DNA methylome was performed as reported previously [12,13]. The miRNA and mRNA expression profiles were exerted by BGI-Shenzhen (Shenzhen, Guangdong, China). The DNA methylome of normal liner tissue and HCC cell lines was aligned (shown on the following UCSC Web site: http://genome.ucsc.edu/cgi-bin/hgTracks?hgS_doOtherUser=submit&hgS_otherUserName=Zhujingde&hgS_otherUserSessionName=LiverCancer_hg19). The other two expression profiles are shown in Tables W2 and W3.

### *Statistical Analysis*

Data are expressed as the mean ± SEM from at least three separate experiments. The data were analyzed with either a two-tailed Student's $t$ test/$\chi^2$ or a one-way analysis of variance for the comparison of more than two groups unless otherwise specified; $P < .05$ was considered significant.

### *Accession Numbers*

Hsa-miR-191: NR_029690.1
TIMP3: NM_000362.4.

## Results

### *miRNA Expression in HCC Is Regulated by DNA Methylation*

To identify the novel DNA methylation regulation of miRNAs in HCC, we ascertained the miRNA expression profile and DNA methylome in normal liver tissues and SMMC-7721, QGY-7703, PLC/PRF/5, BEL-7402, HepG2, and Hep3B cell lines. First, we obtained the locations for all of the miRNAs and CpG islands in the chromosome. If there was a CpG island within 2000 base pairs (bp) of a miRNA gene, that miRNA was chosen as a candidate for DNA methylation regulation; this analysis identified 135 miRNAs. Second, we eliminated the miRNAs that were not expressed (those that had a read value <50) in the HCC cell lines or normal liver tissue from our miRNA expression profile base, which left 31 miRNAs. Third, we checked the DNA methylation status in our DNA methylome data. If there were no differences in DNA methylation between the normal liver tissue and HCC cell lines, the miRNA was eliminated, which left us with 17 miRNAs. Finally, according to our miRNA expression profile, hsa-miR-191 was found to be among the 13 most highly expressed miRNAs in HCC, and its expression level was the highest of the 17 miRNAs in our final analysis. Therefore, we chose miR-191 from the remaining 17 miRNAs (miR-191) for further investigation (Figure 1*A*).

The DNA methylation statuses of 17 miRNAs in the DNA methylome are shown in Figure 1*B*, and the expression levels of these miRs were compared with normal liver tissue in the miRNA expression profile (Figure 1*C*).

### *Relationship between miR-191 Expression in HCC Tissues and Patient Outcomes*

We analyzed 73 pairs of HCC clinical samples and found that the miR-191 levels in the HCC tissues were upregulated by 37.2% compared with adjacent noncancerous tissue. The rate of increased miR-191 expression was 58.9%, and the miR-191 levels in both the HCC tissues and adjacent noncancerous tissues were higher than that of the normal liver tissue (Figure 2*A*).

We placed the samples into two categories based on their miR-191 expression levels in the HCC tissue. The 35 samples with lower expression levels were placed into the low-expression group, and the 35 samples with higher expression levels were placed into the high-expression group. We evaluated the patient survival times after the treatment; these are shown by the survival curve in Figure 2*B*. We

A

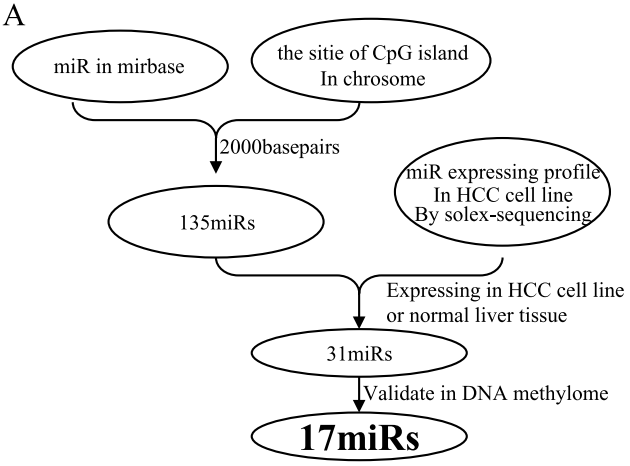


B

| gene name | DNA methylation Fold change (cell mix/NL) |
|---|---|
| miR-10a | 43.00 |
| miR-130b | 3.67 |
| miR-148a | 36.00 |
| miR-191 | 12.00 |
| miR-425 | |
| miR-193a | 5.50 |
| miR-196a-1 | 25.00 |
| miR-210 | 10.50 |
| miR-23b | 6.09 |
| miR-27b | |
| miR-24-1 | |
| miR-26b | 13.00 |
| miR-424 | 9.75 |
| miR-503 | |
| miR-675 | -10.00 |
| miR-886 | 2.54 |
| miR-9-1 | 53.00 |

C

| | SMMC-7721 | QGY-7703 | PLC/PRF/5 | focus |
|---|---|---|---|---|
| hsa-miR-10a | 3.59 | 4.14 | 3.15 | 1.84 |
| hsa-miR-130b | 5.75 | 4.69 | 5.68 | 4.80 |
| hsa-miR-886-5p | 5.63 | 6.68 | 0.00 | 4.70 |
| hsa-miR-193a-5p | 2.81 | -0.29 | 2.48 | 4.41 |
| hsa-miR-210 | 4.92 | 2.39 | 4.37 | 3.50 |
| hsa-miR-92b | 5.33 | 6.30 | 0.36 | 3.17 |
| hsa-miR-24 | 3.22 | 4.94 | 4.05 | 2.98 |
| hsa-miR-152 | 5.28 | 2.41 | 1.58 | 2.82 |
| hsa-miR-193a-3p | 1.94 | -0.97 | 1.53 | 2.62 |
| hsa-miR-191 | 4.16 | 4.32 | 5.26 | 1.90 |
| hsa-miR-886-3p | 2.54 | 4.43 | 0.00 | 1.18 |
| hsa-miR-425 | 2.84 | 3.34 | 5.42 | 1.01 |
| hsa-miR-320a | 2.27 | 2.03 | 1.85 | 0.42 |
| hsa-miR-196a | 7.59 | 6.34 | 3.97 | 0.00 |
| hsa-miR-503 | 5.35 | 4.15 | 3.89 | 0.00 |
| hsa-miR-675 | 0.18 | 5.26 | 0.23 | 0.00 |
| hsa-miR-9 | 0.00 | 1.34 | 4.99 | 0.00 |
| hsa-miR-27b | 0.19 | 1.39 | -0.45 | -1.64 |
| hsa-miR-23b | 0.24 | 1.23 | -0.41 | -1.73 |
| hsa-miR-26b | -0.52 | -0.53 | 0.88 | -1.81 |
| hsa-miR-148a | 0.11 | -0.38 | -2.89 | -3.58 |
| hsa-miR-424 | 0.91 | 0.78 | -0.36 | -4.20 |

**Figure 1.** MicroRNAs are regulated by DNA methylation. (A) Flowchart for the identification of miRNAs that may be regulated by DNA methylation in normal liver tissue and HCC cell lines. The DNA and miRNA samples from normal liver tissue and HCC cells were collected to construct DNA methylome and miRNA expression profiles. To compare the sites of miRNA and CpG islands on the chromosome, a set of 135 miRNAs was first used for analysis. Second, by eliminating the miRNAs that were not expressed in normal tissues or HCC cell lines (based on our miRNA expression profile), we narrowed this set of miRNAs down to 31 miRNAs. Third, we analyzed the differences in methylation signals from these 31 miRNAs between normal tissues and HCC cell lines, further narrowing the set of miRNAs to 17. (B) Differences in DNA methylation between normal tissues and the HCC cell lines in the DNA methylome of 17 miRNAs. (C) Expression profiles of 17 miRNAs in HCC cell lines compared to normal liver tissue. The value shown here is the log (miRNA expression in the HCC cell line/normal liver tissue); data are from miRNA expression profiles.

found that the HCC patients with elevated miR-191 expression had poor prognoses.

miR-191 is an intronic miRNA located in the intron of the *DALRD3* promoter; therefore, we analyzed the expression level of the *DALRD3* mRNA. We found that miR-191 tended to be coexpressed with *DALRD3*. This finding shows that the factors regulating miR-191 expression act at least partially at the transcription level.

*DALRD3*, a miR-191 precursor, and *NDUFAF3* are a *cis*-antisense gene pair (Figure 2*C1*). These genes may be regulated by the same factor (deletion and/or epigenetic modification, for example). We determined the expression levels of these two genes and analyzed the correlations between them and miR-191. We found that miR-191 tended to increase or decrease together with *DALRD3* and *NDUFAF3*, and the *DALRD3* and *NDUFAF3* expression levels were correlated with each other (Figure 2, *C2–C4*).

These results show that the HCC tissues has high miR-191 expression and that patients with high miR-191 expression had poor prognoses. miR-191 tended to be coexpressed with the *cis*-antisense gene pair *DALRD3* and *NDUFAF3*, which implies that miR-191 expression may be regulated by DNA deletion and/or epigenetic modification.

### *Hypomethylation in the First Intron of the hsa-miR-191 Host Gene* DALRD3 *and Increased hsa-miR-191 Expression in an HCC Cell Line*

There is a CpG-rich sequence in the *DALRD3* promoter, and the DNA methylome data shows that a DNA methylation signal is located

in this region (Figure 3*A*). We determined the DNA methylation status of this region using a BSP-based assay; the results indicated that there are DNA methylation differences in the sense strands between the PLC/PRF/5 and Hep3B from normal liver tissue and the SMMC-7721, QGY-7703, BEL-7402, and HepG2 cell lines (Figure 3*B*). The results indicate that the normal liver tissue and these six HCC cell lines could be classified into two types. This region was hypermethylated in the normal liver tissue and in the SMMC-7721, QGY-7703, HepG2, and BEL-7402 cell lines; by contrast, this region was hypomethylated in the PLC/PRF/5 and Hep3B cell lines. No CpGs were methylated in the other 2000-bp sequence that was examined in the *DALRD3* promoter (data not shown).

Next, Northern blot analysis was used to assess the hsa-miR-191 expression in the normal liver tissue and six HCC cell lines (Figure 3*C*). hsa-miR-191 was highly expressed in the HCC cell lines, especially PLC/PRF/5 and Hep3B (Figure 3*C*, *lanes 4* and *7*). In addition, qRT-PCR revealed that the *DALRD3* and *NDUFAF3* mRNA levels were upregulated in PLC/PRF/5 and Hep3B compared with the normal liver tissue and the other four cell lines (Figure 3, *D* and *E*).

Together, the results of these assays showed that there was hypomethylation at the hsa-miR-191 locus and that its expression (and the expression of its host gene) was correlated in the normal liver tissue and six HCC cell lines.

### *DNA Methylation Status of the miR-191 Locus and miR-191 Expression in BEL-7402 Cells after Treatment with 5-Aza-CdR*

To confirm the correlation between the hsa-miR-191 DNA methylation status and the hsa-miR-191 expression levels, we used BEL-7402

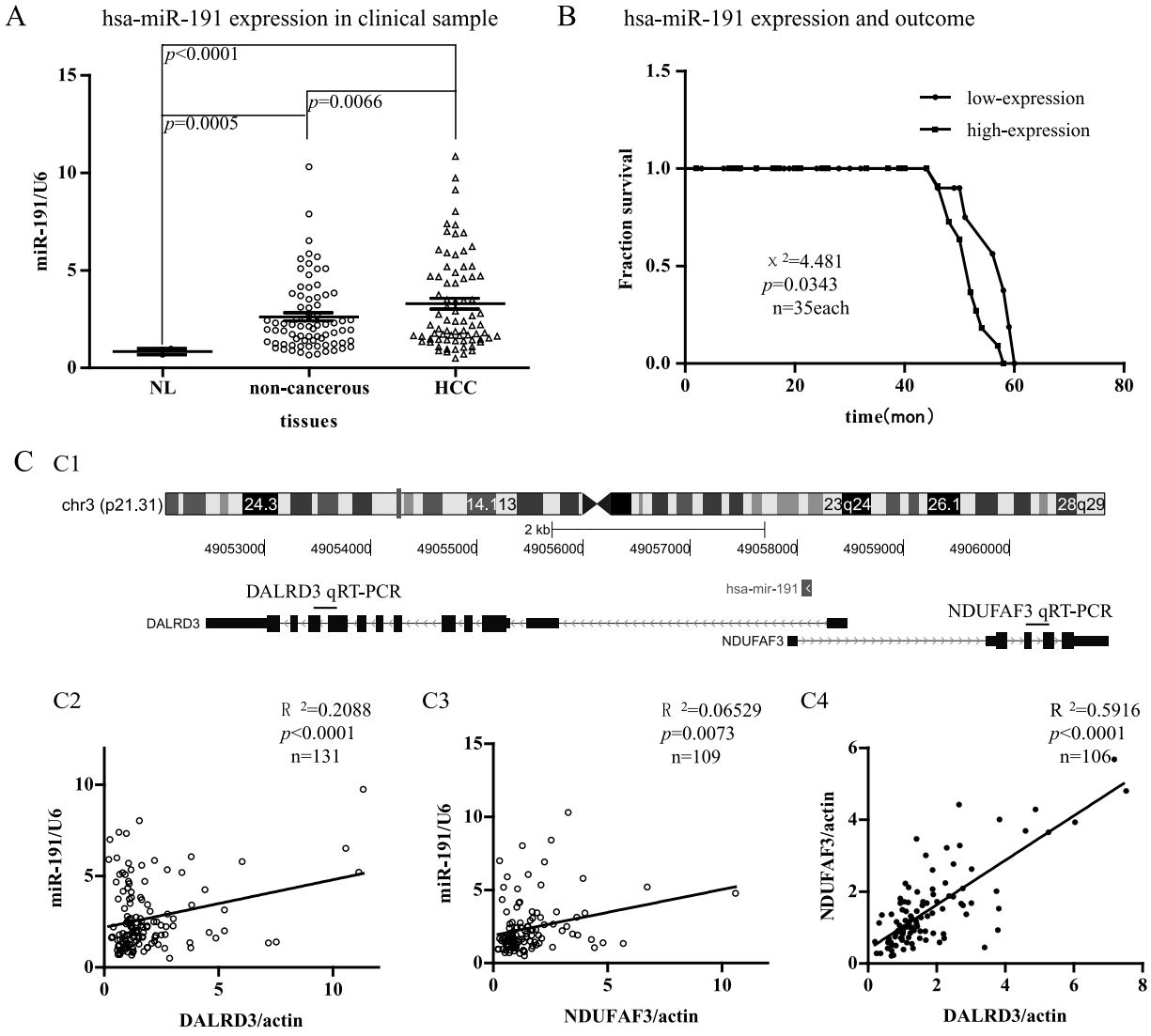


**Figure 2.** The high expression level of miR-191 in HCC tissues is associated with a poor prognosis. (A) We analyzed the expression levels of miRNAs in 73 pairs of HCC tissues and found an increase of 37.2% in the expression level of miR-191 in HCC tissues when compared with adjacent noncancerous tissues, $P = .0066$ (paired $t$ test). miR-191 expression is upregulated in 58.9% of these 73 pairs of tissues. The expression levels of miR-191 are higher in both HCC tissues and adjacent noncancerous tissues compared with normal tissues. (B) Overexpression of miR-191 is associated with a poor prognosis. miR-191 expression in HCC tissues is listed from lowest to highest; the 35 HCC tissues with the lowest miR-191 expression levels were placed into the low-expression group, whereas the 35 HCC tissues with the highest miR-191 expression levels were placed into the high-expression group. (C) The miR-191 precursors, *DALRD3* and *NDUFAF3*, a *cis*-antisense gene pair, tend to be coexpressed.

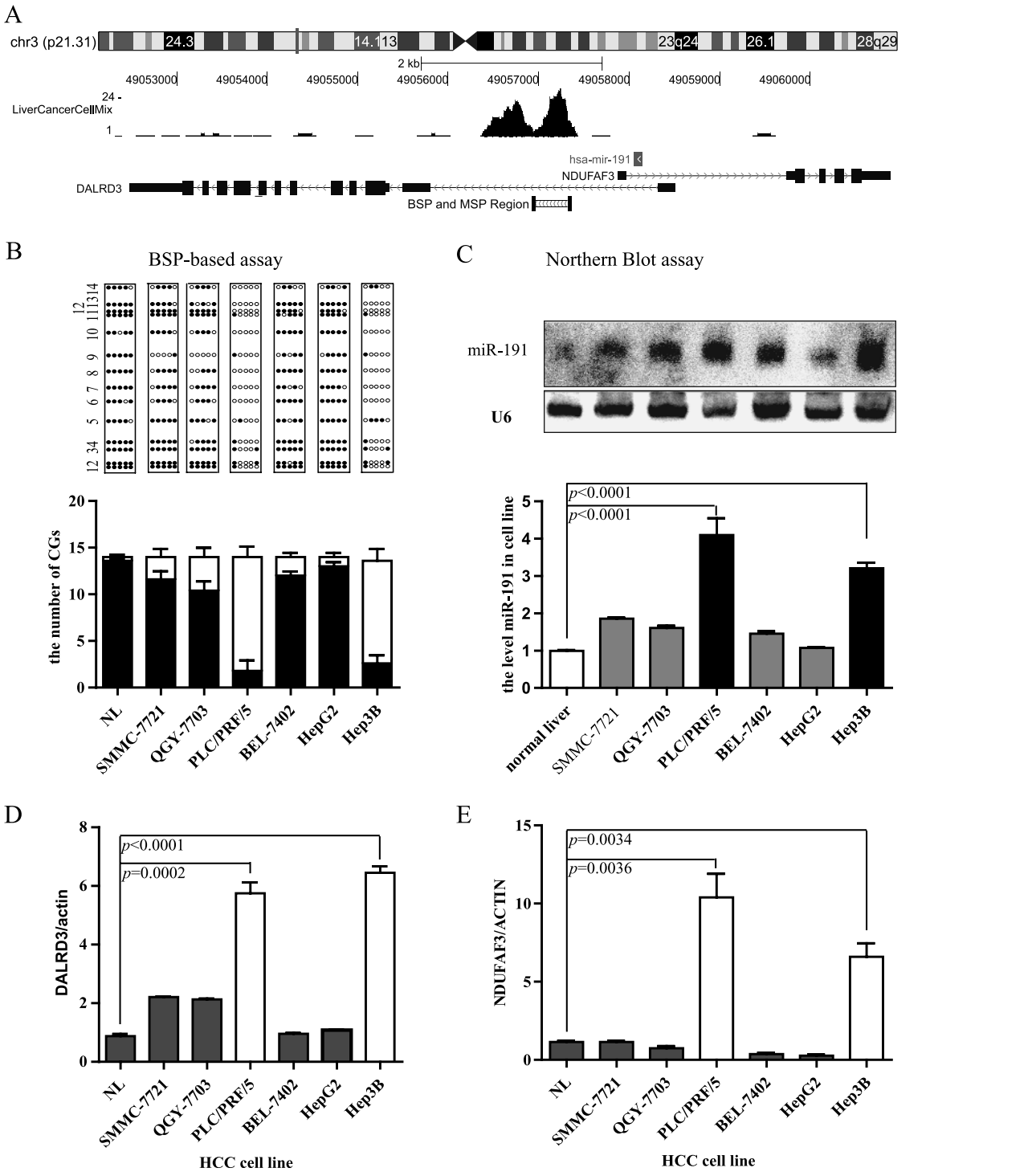


**Figure 3.** Some cells show hypomethylation of the hsa-miR-191 locus and high expression of hsa-miR-191. (A) The miRNA hsa-miR-191 is located in the promoter region of DALRD3 on chromosome 3, where there is also a CpG-rich sequence and a DNA methylation signal. In addition, BSP and MSP regions are located in the first intron of DALRD3, downstream of hsa-miR-191. (B) The hypomethylation of hsa-miR-191 in HCC cells is shown by a BSP-based assay. The levels of DNA methylation are 92.9%, 82.9%, 84.3%, 12.9%, 85.7%, 92.9%, and 18.6% in normal liver tissue, SMMC-7721 cells, QGY-7703, PLC/PRF/5, BEL-7402, HepG2, and Hep3B cells, respectively. (C) hsa-miR-191 expression levels in normal liver tissue and HCC cell lines by Northern blot. The quantification of hsa-miR-191 expression is shown based on the results of a Northern blot assay. The expression level of hsa-miR-191 was normalized to that of U6. The expression levels were upregulated 4.1-fold ($P < .0001$) and 3.21-fold ($P < .0001$) in PLC/PRF/5 and Hep3B cell lines, respectively, compared with the levels of normal liver tissue. (D, E) mRNA levels of *DALRD3* (D) and *NDUFAF3* (E) in normal liver tissue and HCC cell lines were analyzed by qRT-PCR. These two genes were highly expressed in PLC/PRF/5 and Hep3B cell lines. These results were analyzed by a Student's *t* test.

as a model because the hsa-miR-191 locus is almost completely methylated and the expression level of hsa-miR-191 is low in these cells.

In the BEL-7402 cell line, the rate of DNA methylation decreased from 84.3% to 71%, 51%, and 27% after 1-, 2-, and 5-day treatments, respectively, with 5-aza-CdR (Figure 4*A*). The Northern blot analysis and qRT-PCR assays revealed that the hsa-miR-191 expression in the 5-aza-CdR–treated BEL-7402 cells was upregulated (Figure 4, *B1* and *B2*) compared with the untreated controls. The same results were seen in independent triplicate assays. We obtained similar results for the SMMC-7721 cells (data not shown). In the BEL-7402 cell line, the addition of trichostatin A (TSA), which specifically inhibits mammalian histone deacetylase, 24 hours after the 5-day 5-aza-CdR treatment did not alter the hsa-miR-191 expression compared with the expression levels of the trichostatin A–untreated controls (data not shown). We also analyzed the *DALRD3* and *NDUFAF3* mRNA expression levels and found that these two genes were upregulated after treatment (Figure 4, *B2* or *B3*).

These results show that when 5-aza-CdR demethylates the sequence in the hsa-miR-191 locus, hsa-miR-191 and its host gene are upregulated. Therefore, DNA methylation is able to regulate hsa-miR-191 expression.

### *hsa-miR-191 Locus Methylation in HCC Primary Tumors and Its Clinicopathologic Correlation*

We analyzed hsa-miR-191 locus methylation in the 11 pairs of HCC primary tumors; the results of this analysis are shown in Figure 5*A*. All of the DNA was hypomethylated in these HCC samples and hypermethylated in their adjacent tissues. The miR-191 expression was correlated with methylation status in these samples (Figure 5*B*).

Samples 257 and 202 were chosen to validate the DNA methylation status using the BSP-based assay. The results verified that there was hypomethylation in the HCC samples and hypermethylation in their adjacent tissues (Figure 5*C*).

Next, we analyzed the 73 clinical HCC samples; the results of this analysis are shown in Table W4, which shows that the hypomethylation rate was 63.0%. We placed these samples into two categories: a hypomethylation group and a hypermethylation group. The miR-191 expression levels in these two groups is shown in Figure 5*D*, which indicates that the miR-191 expression was higher in the hypomethylated group than in the hypermethylated group.

This result shows that the hypomethylation at the hsa-miR-191 locus was correlated with its expression in the clinical samples.

### *Overexpression of hsa-miR-191 Induces SMMC-7721 Cells to Transition into Mesenchymal-like Cells*

We examined the cell morphology, epithelial and mesenchymal markers, and cell migration and invasion in stable hsa-miR-191–overexpressing cells.

First, an SMMC-7721 cell line that stably overexpressed hsa-miR-191 was developed using a lentiviral-packed vector containing the hsa-miR-191 precursor. By a qRT-PCR analysis, the two stably overexpressing

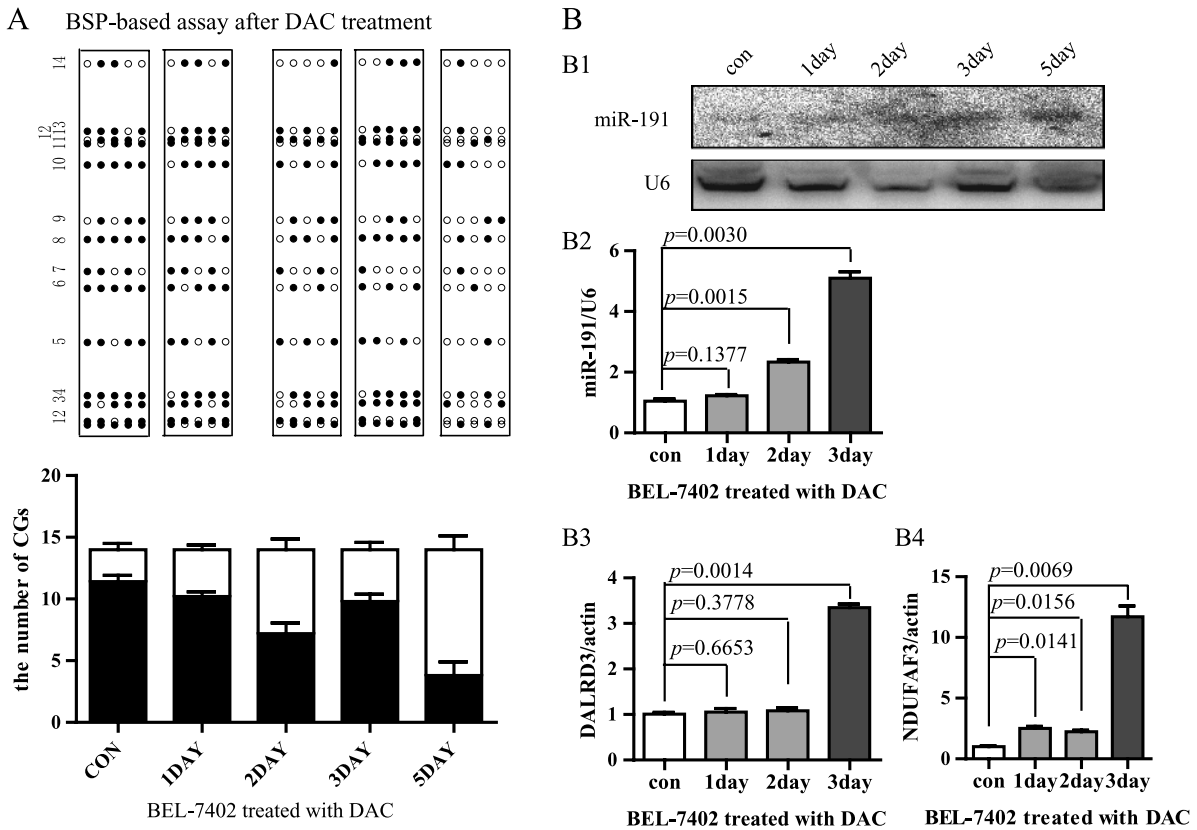


**Figure 4.** Alterations in DNA methylation status and hsa-miR-191 expression in BEL-7402 cells that were treated with 5′-aza-CdR. (A) The hsa-miR-191 locus becomes hypomethylated after 5′-aza-CdR treatment. In BEL-7402 cells, the rate of DNA methylation before treatment was 84.3% and decreased to 71%, 51%, 70%, and 27% after 1, 2, 3, and 5 days of treatment, respectively. (B) The levels of miR-191 expression (B1, B2) and the mRNA levels of *DALRD3*/*NDUFAF3* (B3, B4) are upregulated after treatment with 5′-aza-CdR. The expression level of miR-191 was detected by Northern blot and qRT-PCR, and the mRNA levels of *DALRD3*/*NDUFAF3* were detected by qRT-PCR.

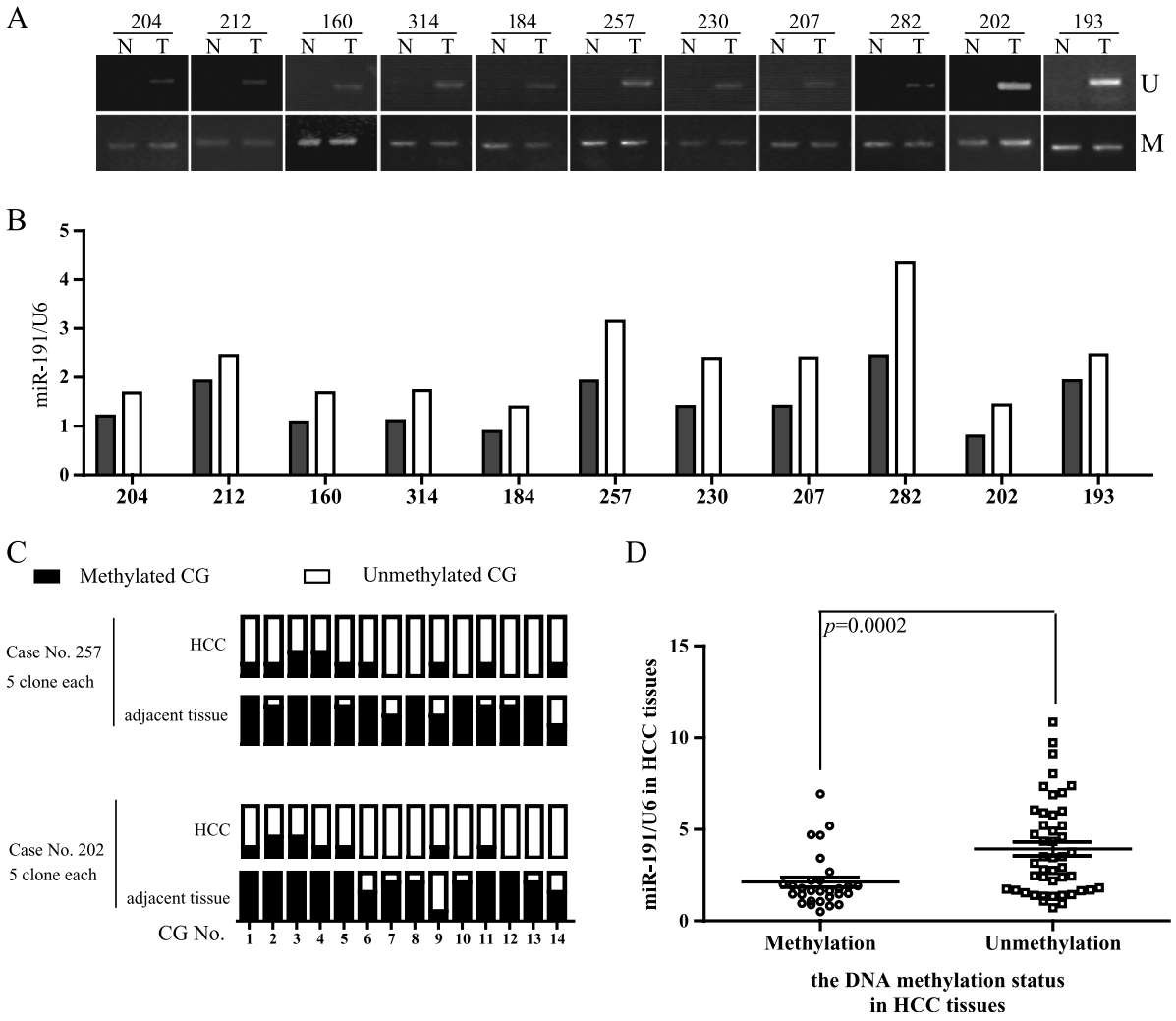


**Figure 5.** The hsa-miR-191 locus is hypomethylated and highly expressed in HCC tissues. (A) An MSP-based assay was used to detect hsa-miR-191 locus methylation in 11 pairs of clinical HCC tissues. No methylation of the hsa-miR-191 locus was observed in 11 HCC tissues. (B) hsa-miR-191 is highly expressed in the 11 HCC tissues that were not methylated. (C) Validation of the MSP-based assay by the BSP-based assay. Case nos. 257 and 202 were chosen for the assay. Hypermethylation was observed in adjacent noncancerous tissues, and hypomethylation was observed in HCC tissues. (D) An MSP-based assay was used to detect methylation of the hsa-miR-191 locus in 73 clinical HCC tissues. On the basis of these results, the clinical tissues were placed into two categories, a methylated group and a nonmethylated group. The expression level of hsa-miR-191 in the nonmethylated group was higher than the expression level in the methylated group (2.1-fold difference). The rate of hypomethylation was 63.0%. The results were analyzed by a Student's *t* test.

**Figure 6.** Overexpression of hsa-miR-191 induces SMMC-7721 cells to transition into mesenchymal-like cells. (A) Expression levels of hsa-miR-191 in the hsa-miR-191 stably overexpressing cell line, as detected by qRT-PCR. The expression levels of hsa-miR-191 were upregulated approximately four-fold in the two resultant clones. (B) Alterations in epithelial (cytokeratin and E-cadherin) and mesenchymal (vimentin and N-cadherin) marker expression in the stable hsa-miR-191–overexpressing cell lines compared with the control. The expression levels of the epithelial markers pan-cytokeratin and E-cadherin were sharply reduced. By contrast, the expression levels of the mesenchymal markers vimentin and N-cadherin were increased in the hsa-miR-191–overexpressing cell lines. (C) The overexpression of hsa-miR-191 leads to an increase in cell migration. As determined by the scratch assay, the hsa-miR-191–overexpressing cell lines reached 87% fusion 8 days after the scratch-induced wound compared with the control (stable overexpression of the empty vector; $P = .0141$ and $P = .0045$ in the stable hsa-miR-191–overexpressing cell lines 1 and 2, respectively). By contrast, the SMMC-7721 control cell line reached 59.0% fusion. (D) Morphology of the stable hsa-miR-191–overexpressing cell line compared with the morphology of the control cell line. The overexpressing cells have long, thin processes and reduced cell-to-cell contacts. (E and F) Overexpression of hsa-miR-191 increased cell invasion as determined by the transwell assay using a Matrigel-coated membrane. Cell invasion increased by 2.02-fold ($P = .0028$) and 1.72-fold ($P = .0045$) in the stable hsa-miR-191 overexpressing cell lines 1 and 2, respectively, compared with the control. Results were analyzed by a Student's *t* test.

cell lines were shown to have a four-fold up-regulation of hsa-miR-191 expression (Figure 6*A*). The cell morphology of the stable cell line was significantly altered (Figure 6*D*); the cells had long and thin processes, cell-to-cell contraction was reduced, and their adhesion to the plate was reduced; therefore, we cultured the cell line on poly-L-lysine–precoated plates.

Next, the epithelial and mesenchymal cell marker expression levels were examined in the stable cell lines and in the control cell line by Western blot. In the stable hsa-miR-191–overexpressing cell lines, the epithelial cell markers pan-cytokeratin and E-cadherin were suppressed, and the mesenchymal cell markers vimentin and N-cadherin were upregulated (Figure 6*B*).

To further evaluate hsa-miR-191 function in the liver cells, the effect of stable hsa-miR-191 overexpression on the invasion and migration of the SMMC-7721 cells was studied. The invasion assay revealed that the cell invasion capacity of the stable hsa-miR-191–overexpressing

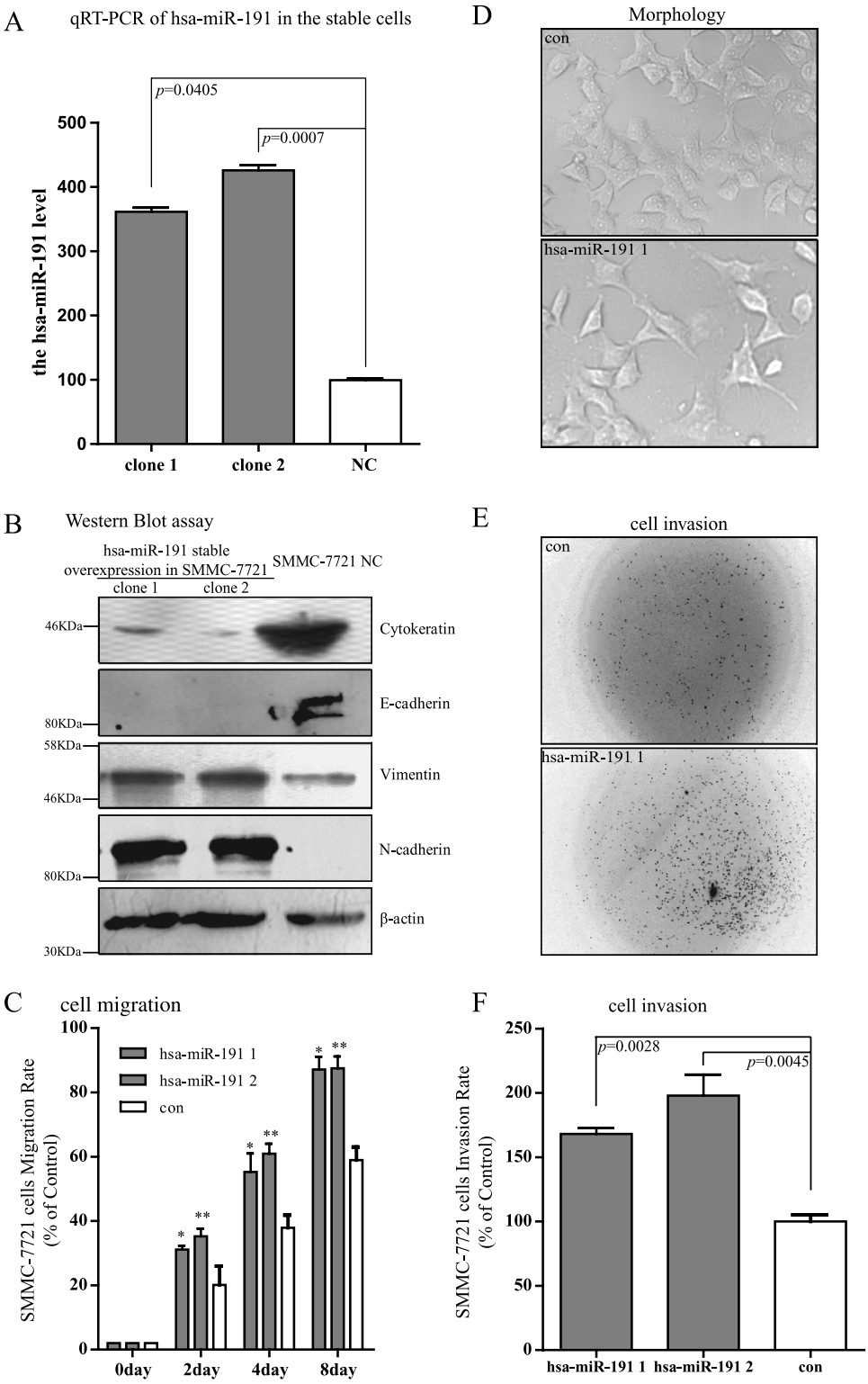

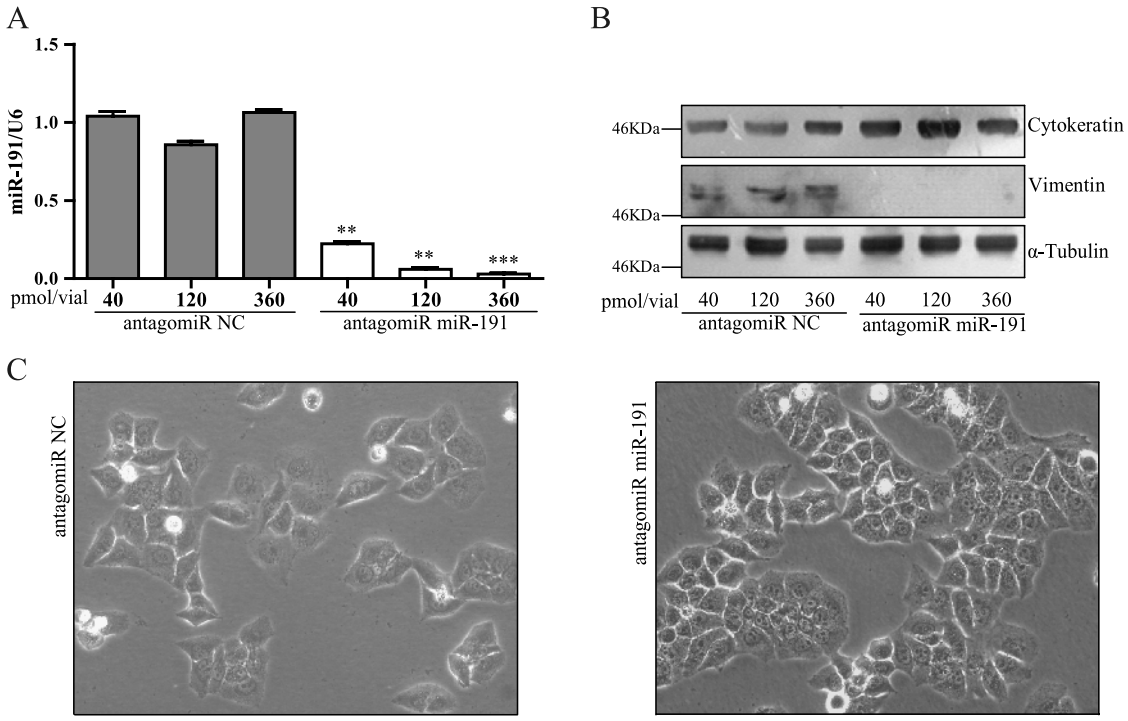


**Figure 7.** Inhibition of hsa-miR-191 induces SMMC-7721 cells to transition into epithelial-like cells. (A) Expression levels of hsa-miR-191 in the SMMC-7721 cell line transfected with antagomiR to miR-191, as detected by qRT-PCR. Expression levels of hsa-miR-191 were downregulated ($P = .0026$, $P = .0016$, and $P = .0006$ in the SMMC-7721 cells transfected with antagomiR to miR-191 [40, 120, and 360 pmol, respectively] compared with their NC controls, Student's *t* test). (B) Alterations in epithelial (cytokeratin) and mesenchymal (vimentin) marker expression in the SMMC-7721 cells transfected with antagomiR-191 compared with the controls. The expression level of the pan-cytokeratin epithelial marker was increased. By contrast, the expression level of the mesenchymal marker vimentin was suppressed. (C) The morphology of the SMMC-7721 cells that were transfected with antagomiR to miR-191 is altered. The cell-to-cell contraction is increased in the SMMC-7721 cells that were transfected with antagomiR to miR-191 compared with the controls.

cell lines was increased by more than 60% (Figure 6, *E* and *F*), and the wound healing assay revealed that the migration capacity of these cells was also increased (Figure 6*C*).

### *Inhibition of hsa-miR-191 Induces SMMC-7721 Cells to Transition to Epithelial-Like Cells*

We transiently transfected antagomiR to miR-191 into the SMMC-7721 cell line with Amaxa Nucleofector, with a transfection efficiency of 100% (using cotransfection with GFP as an indicator). The miR-191 level was detected by qRT-PCR to confirm the efficiency of the antagomiR, and it was significantly downregulated (Figure 7*A*).

The epithelial and mesenchymal cell marker expression levels were then examined by Western blot assay in the SMMC-7721 cells that were transfected with antagomiR to miR-191 or to NC. In the SMMC-771 cells that were transfected with antagomiR to miR-191, the pan-cytokeratin epithelial cell marker was upregulated compared with the SMMC-7721 transfected with antagomiR to NC; conversely, the level of the mesenchymal cell marker vimentin was reduced (Figure 7*B*).

The cell morphology of the SMMC-7721 cells that were transfected to miR-191 was significantly altered (Figure 7*C*), and the cell-to-cell contraction was increased (Figure 7*C*).

Taken together, these *in vitro* results indicate that the hsa-miR-191 stable SMMC-7721 cell line had mesenchymal features, including long and thin processes, loss of adhesion, reduced cell-to-cell contraction, and increased cell migration and invasion. In addition, inhibiting the miR-191 expression in the SMMC-7721 cell line resulted in epithelial features, including altered marker expression and increased cell-to-cell contraction.

### *hsa-miR-191 Directly Suppresses TIMP3 Expression*

Identifying the hsa-miR-191 target genes is essential to better understand its biologic functions. First, we obtained a prediction collection from miRNA.org. Second, we obtained two collections from our mRNA microarray data: one that was highly expressed in normal tissue, with low expression levels in PLC/PRF/5; and one that was highly expressed in the SMMC-7721 cell line and had low expression levels in PLC/PRF/5. Third, we compared these data to the data obtained from miRNA.org; the common genes from these two sources represented the target genes (Figure 8*A*).

According to their mRNA expression profiles (Figure 8*B*), *TIMP3*, *AUTS2* (autism susceptibility candidate 2), *LTBP1* (latent transforming growth factor beta-binding protein 1), *PLOD2* (procollagen-lysine, 2-oxoglutarate 5-dioxygenase 2), *LIMCH1* (LIM and calponin homology domains 1), *NFIA* (nuclear factor I/A), *BASP1* (brain abundant, membrane attached signal protein 1), *PCSK9* (proprotein convertase subtilisin/kexin type 9), and *SORL1* (sortilin-related receptor, L [DLR class] A repeat containing) were candidates for the miR-191 targets. We analyzed one of these candidates: *TIMP3*. The *TIMP3* mRNA level in the normal tissue and six cell lines is shown in Figure 8*C*; the PLC/PRF/5 and Hep3B cell lines had the lowest *TIMP3* mRNA expression levels. We placed the predicted miR-191 target sequence (Figure W1)

into the 3′UTR of luciferase, and the luciferase activity was downregulated when the miR-191 mimics were cotransfected (Figure 8*D*). We then checked the TIMP3 protein levels in the stable SMMC-7721 cell lines, which indicated that miR-191 could induce decreased expression of the TIMP3 protein (Figure 8*E*).

Together, these results show that hsa-miR-191 can target *TIMP3* mRNA and suppress TIMP3 protein expression.

## Discussion

The emergence of next-generation sequencing of bisulfite-converted DNA represents an important advance in the field of DNA methylation analysis [12–16]. This technology has enabled human methylome analysis to advance from single chromosomes [17] to low- (100-bp) resolution complete genomes to single-base resolution complete genomes [18]. Using this technology, we obtained the DNA methylomes of normal liver tissue and HCC cell lines to analyze the DNA methylation status in HCC more carefully. In our study, we found that 13 CpG-rich regions may regulate 17 miRNAs. Only seven miRs have been reported in oncology research to be upregulated by DNA methylation; one of these seven miRs, miR-148a, has been reported to be regulated by DNA methylation in HCC. We found that miR-193a regulation by DNA methylation in HCC (unpublished data) can be validated by these data, and we investigated other miRNAs in this manner.

miRNA expression can be regulated at the level of expression or splicing [19]. At the transcriptional level, the factors that regulate gene expression are transcription factors, DNA deletion, and epigenetic mechanisms. However, the gene structure of miR-191 is a special *cis*-antisense gene structural pair. Gene transcription in this structure may be regulated by DNA deletion or by epigenetic mechanisms [20].

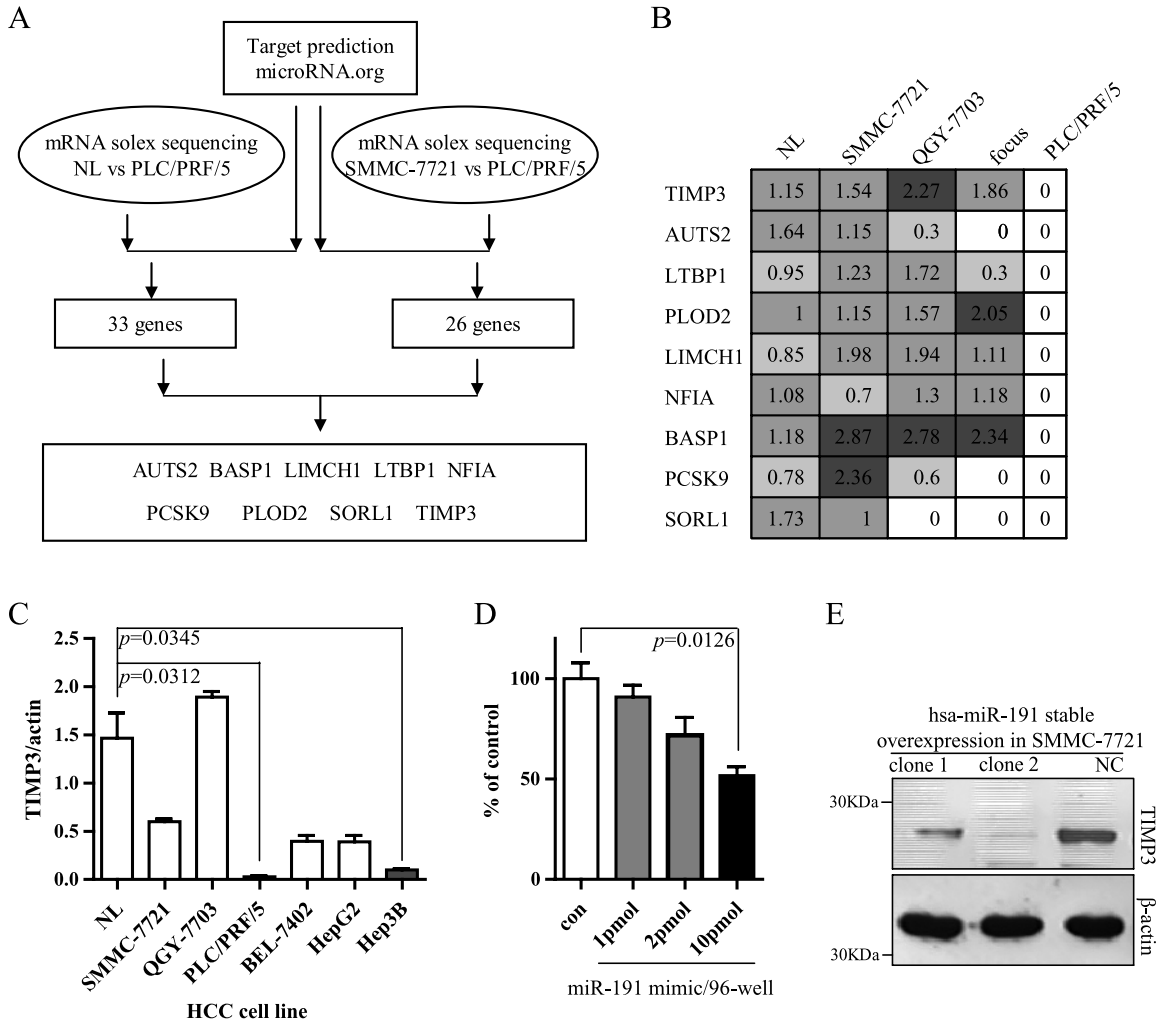


**Figure 8.** Analysis of hsa-miR-191 targets. (A) Flowchart of hsa-miR-191 target analysis. The target analysis is based on the miR-191 expression level in HCC cell lines (Figure 2), mRNA expression profile (our unpublished data), and target prediction in microRNA.org. Nine genes were chosen as putative miR-191 targets. (B) mRNA profiles of the nine target genes in the HCC cell lines. The value is the log (mRNA expression in HCC cell line/normal liver tissue) according to the mRNA expression profile. (C) TIMP3 has low expression in the HCC cell lines. TIMP3 has especially low expression in the PLC/PRF/5 and Hep3B cell lines. (D) Reduced firefly luciferase activity owing to hsa-miR-191 expression. SMMC-7721 was cotransfected with hsa-miR-191 mimics and a reporter construct that carried a miR-191 prediction target sequence in TIMP3; the activity of firefly luciferase was normalized to that of *Renilla* luciferase. Compared with the control, the activity of firefly luciferase was reduced by 50% when the level of hsa-miR-191 was increased to 10 pmol/well (96-well plate). (E) Reduction in TIMP3 protein levels in stable hsa-miR-191–overexpressing cell lines. Compared with the control, TIMP3 levels were reduced by 50% to 80% in both stable hsa-miR-191–overexpressing cell lines.

In our study, we found that elevated miR-191 expression was associated with hypomethylation at the miR-191 locus, both in the HCC cell lines and clinical samples. The 5-aza-DAC demethylation agent induced miR-191 locus demethylation and upregulated the expression levels of miR-191 and its host gene. According to our data, the correlation between the expression of miR-191 and that of its host gene (*DALRD3*) is not perfect because the miR-191 and *DALRD3* expression may be regulated by other factors. However, the miR-191 expressions in both the HCC cell lines and clinical HCC samples were correlated with the DNA methylation status, and the demethylation agent induced HCC cell line demethylation at the hsa-miR-191 locus, resulting in the up-regulation of hsa-miR-191 expression. Therefore, we concluded that the difference in DNA methylation status in normal tissue, HCC cell lines, and clinical HCC samples is an important mechanism underlying the differences in miR-191 expression in these samples.

Some miRNAs can induce an epithelial-to-mesenchymal transition or mesenchymal-to-epithelial transition [21,22]. One of these, hsa-miR-191, is an important miRNA that has been the focus of extensive research. Some toxins (5-FU, dioxin and cigarette smoke, for example) cause miR-191 deregulation [23–25]. In oncology research, increased miR-191 expression has been reported in malignant melanoma, acute myeloid leukemia, breast cancer, ovarian cancer, and colorectal cancer; this high expression may be associated with poor prognosis [26–33]. High hsa-miR-191 expression has also been reported in HCC [24]. In this study, we confirmed that miR-191 expression is associated with poor prognosis in HCC and that DNA methylation is the factor that causes increased miR-191 expression in HCC.

In our study, we identified nine genes (*TIMP3*, *AUTS2*, *LTBP1*, *PLOD2*, *LIMCH1*, *NFIA*, *BASP1*, *PCSK9*, and *SORL1*) as miR-191 candidate target genes from their baseline expression levels in the normal tissue and HCC cell lines. *TIMP3* plays a functional role in the lysophosphatidic acid (LPA)–induced invasion [34], and miR-21/miR-221 and 222 can also regulate *TIMP3* expression [35,36]. *LTBP1* has been shown to regulate transforming growth factor-β activation and regulate cancer metastasis and extracellular matrix accumulation [37,38]. *PLOD2* has been reported to be a telopeptide lysyl hydroxylase, which is an important enzyme in fibrosis [39]. *NFIA* can regulate cell differentiation [40,41], and increased expression of *NFIA* is associated with improved survival [42]. *BASP1* is a weakly expressed gene in HCC [43] that has been identified as a tumor suppressor [44] and a regulator of differentiation [45]. *PCSK9* is involved in lipid metabolism [46]. *LIMCH1* and *SORL1* are involved in metal ion transport/binding [47,48]. *AUTS2* has been identified in the regulation of alcohol consumption. Thus, five of these nine genes are involved in oncology research and are mainly associated with metastasis and differentiation; these genes may also be involved in miR-191 function in hepatic carcinogenesis. The other genes may be associated with metabolism or metal ion transport/binding, or they may be involved in miR-191 function in normal liver tissue.

In conclusion, our results suggest that DNA hypomethylation can cause increased hsa-miR-191 expression in HCC cells and HCC tissues and that this high expression is associated with poor prognosis. Overexpression of hsa-miR-191 induced the SMMC-7721 cell line to develop mesenchymal-like cell features (e.g., reduced cell-cell contract, the appearance of long and thin processes, and increased cell migration and invasion). hsa-miR-191 exerts these functions by targeting nine genes. These findings may facilitate developing potential HCC therapeutics.

## Acknowledgments

The authors thank Zhu Jingde at the Shanghai Cancer Institute for the DNA methylome, miRNA, and mRNA expression profiles.

## References

[1] El-Serag HB and Rudolph KL (2007). Hepatocellular carcinoma: epidemiology and molecular carcinogenesis. *Gastroenterology* **132**, 2557–2576.
[2] Calvisi DF, Ladu S, Gorden A, Farina M, Lee JS, Conner EA, Schroeder I, Factor VM, and Thorgeirsson SS (2007). Mechanistic and prognostic significance of aberrant methylation in the molecular pathogenesis of human hepatocellular carcinoma. *J Clin Invest* **117**, 2713–2722.
[3] Nomoto S, Kinoshita T, Kato K, Otani S, Kasuya H, Takeda S, Kanazumi N, Sugimoto H, and Nakao A (2007). Hypermethylation of multiple genes as clonal markers in multicentric hepatocellular carcinoma. *Br J Cancer* **97**, 1260–1265.
[4] Morgan TR, Mandayam S, and Jamal MM (2004). Alcohol and hepatocellular carcinoma. *Gastroenterology* **127**, S87–S96.
[5] Bartel DP (2004). MicroRNAs: genomics, biogenesis, mechanism, and function. *Cell* **116**, 281–297.
[6] He L and Hannon GJ (2004). MicroRNAs: small RNAs with a big role in gene regulation. *Nat Rev Genet* **5**, 522–531.
[7] Calin GA and Croce CM (2006). MicroRNA signatures in human cancers. *Nat Rev Cancer* **6**, 857–866.
[8] Datta J, Kutay H, Nasser MW, Nuovo GJ, Wang B, Majumder S, Liu CG, Volinia S, Croce CM, Schmittgen TD, et al. (2008). Methylation mediated silencing of microRNA-1 gene and its role in hepatocellular carcinogenesis. *Cancer Res* **68**, 5049–5058.
[9] Furuta M, Kozaki KI, Tanaka S, Arii S, Imoto I, and Inazawa J (2010). miR-124 and miR-203 are epigenetically silenced tumor-suppressive microRNAs in hepatocellular carcinoma. *Carcinogenesis* **31**, 766–776.
[10] Yu J, Zhu T, Wang Z, Zhang H, Qian Z, Xu H, Gao B, Wang W, Gu L, Meng J, et al. (2007). A novel set of DNA methylation markers in urine sediments for sensitive/specific detection of bladder cancer. *Clin Cancer Res* **13**, 7296–7304.
[11] Xu T, Zhu Y, Wei QK, Yuan Y, Zhou F, Ge YY, Yang JR, Su H, and Zhuang SM (2008). A functional polymorphism in the *miR-146a* gene is associated with the risk for hepatocellular carcinoma. *Carcinogenesis* **29**, 2126–2131.
[12] Li Y, Zhu J, Tian G, Li N, Li Q, Ye M, Zheng H, Yu J, Wu H, Sun J, et al. (2010). The DNA methylome of human peripheral blood mononuclear cells. *PLoS Biol* **8**, e1000533.
[13] Xiang H, Zhu J, Chen Q, Dai F, Li X, Li M, Zhang H, Zhang G, Li D, Dong Y, et al. (2010). Single base-resolution methylome of the silkworm reveals a sparse epigenomic map. *Nat Biotechnol* **28**, 516–520.
[14] Cokus SJ, Feng S, Zhang X, Chen Z, Merriman B, Haudenschild CD, Pradhan S, Nelson SF, Pellegrini M, and Jacobsen SE (2008). Shotgun bisulphite sequencing of the *Arabidopsis* genome reveals DNA methylation patterning. *Nature* **452**, 215–219.
[15] Lister R, O'Malley RC, Tonti-Filippini J, Gregory BD, Berry CC, Millar AH, and Ecker JR (2008). Highly integrated single-base resolution maps of the epigenome in *Arabidopsis*. *Cell* **133**, 523–536.
[16] Meissner A, Mikkelsen TS, Gu H, Wernig M, Hanna J, Sivachenko A, Zhang X, Bernstein BE, Nusbaum C, Jaffe DB, et al. (2008). Genome-scale DNA methylation maps of pluripotent and differentiated cells. *Nature* **454**, 766–770.
[17] Eckhardt F, Lewin J, Cortese R, Rakyan VK, Attwood J, Burger M, Burton J, Cox TV, Davies R, Down TA, et al. (2006). DNA methylation profiling of human chromosomes 6, 20 and 22. *Nat Genet* **38**, 1378–1385.
[18] Down TA, Rakyan VK, Turner DJ, Flicek P, Li H, Kulesha E, Graf S, Johnson N, Herrero J, Tomazou EM, et al. (2008). A Bayesian deconvolution strategy for immunoprecipitation-based DNA methylome analysis. *Nat Biotechnol* **26**, 779–785.
[19] Winter J, Jung S, Keller S, Gregory RI, and Diederichs S (2009). Many roads to maturity: microRNA biogenesis pathways and their regulation. *Nat Cell Biol* **11**, 228–234.
[20] Grinchuk OV, Jenjaroenpun P, Orlov YL, Zhou J, and Kuznetsov VA (2010). Integrative analysis of the human cis-antisense gene pairs, miRNAs and their transcription regulation patterns. *Nucleic Acids Res* **38**, 534–547.
[21] Cowden Dahl KD, Dahl R, Kruichak JN, and Hudson LG (2009). The epidermal growth factor receptor responsive miR-125a represses mesenchymal morphology in ovarian cancer cells. *Neoplasia* **11**, 1208–1215.
[22] Meng Z, Fu X, Chen X, Zeng S, Tian Y, Jove R, Xu R, and Huang W (2010). miR-194 is a marker of hepatic epithelial cells and suppresses metastasis of liver cancer cells in mice. *Hepatology* **52**, 2148–2157.

[23] Zhou J, Zhou Y, Yin B, Hao W, Zhao L, Ju W, and Bai C (2010). 5-Fluorouracil and oxaliplatin modify the expression profiles of microRNAs in human colon cancer cells *in vitro*. *Oncol Rep* **23**, 121–128.

[24] Elyakim E, Sitbon E, Faerman A, Tabak S, Montia E, Belanis L, Dov A, Marcusson EG, Bennett CF, Chajut A, et al. (2010). hsa-miR-191 is a candidate oncogene target for hepatocellular carcinoma therapy. *Cancer Res* **70**, 8077–8087.

[25] Izzotti A, Calin GA, Arrigo P, Steele VE, Croce CM, and De Flora S (2009). Downregulation of microRNA expression in the lungs of rats exposed to cigarette smoke. *FASEB J* **23**, 806–812.

[26] Caramuta S, Egyhazi S, Rodolfo M, Witten D, Hansson J, Larsson C, and Lui WO (2010). MicroRNA expression profiles associated with mutational status and survival in malignant melanoma. *J Invest Dermatol* **130**, 2062–2070.

[27] Garzon R, Volinia S, Liu CG, Fernandez-Cymering C, Palumbo T, Pichiorri F, Fabbri M, Coombes K, Alder H, Nakamura T, et al. (2008). MicroRNA signatures associated with cytogenetics and prognosis in acute myeloid leukemia. *Blood* **111**, 3183–3189.

[28] Hui AB, Shi W, Boutros PC, Miller N, Pintilie M, Fyles T, McCready D, Wong D, Gerster K, Waldron L, et al. (2009). Robust global micro-RNA profiling with formalin-fixed paraffin-embedded breast cancer tissues. *Lab Invest* **89**, 597–606.

[29] Kent OA, Mullendore M, Wentzel EA, Lopez-Romero P, Tan AC, Alvarez H, West K, Ochs MF, Hidalgo M, Arking DE, et al. (2009). A resource for analysis of microRNA expression and function in pancreatic ductal adenocarcinoma cells. *Cancer Biol Ther* **8**, 2013–2024.

[30] Leite KR, Tomiyama A, Reis ST, Sousa-Canavez JM, Sanudo A, Dall'Oglio MF, Camara-Lopes LH, and Srougi M (2011). MicroRNA-100 expression is independently related to biochemical recurrence of prostate cancer. *J Urol* **185**, 1118–1122.

[31] Shen J, DiCioccio R, Odunsi K, Lele SB, and Zhao H (2010). Novel genetic variants in miR-191 gene and familial ovarian cancer. *BMC Cancer* **10**, 47.

[32] Xi Y, Formentini A, Chien M, Weir DB, Russo JJ, Ju J, and Kornmann M (2006). Prognostic values of microRNAs in colorectal cancer. *Biomark Insights* **2**, 113–121.

[33] Wynendaele J, Bohnke A, Leucci E, Nielsen SJ, Lambertz I, Hammer S, Sbrzesny N, Kubitza D, Wolf A, Gradhand E, et al. (2010). An illegitimate microRNA target site within the 3′ UTR of MDM4 affects ovarian cancer progression and chemosensitivity. *Cancer Res* **70**, 9641–9649.

[34] Sengupta S, Kim KS, Berk MP, Oates R, Escobar P, Belinson J, Li W, Lindner DJ, Williams B, and Xu Y (2007). Lysophosphatidic acid downregulates tissue inhibitor of metalloproteinases, which are negatively involved in lysophosphatidic acid–induced cell invasion. *Oncogene* **26**, 2894–2901.

[35] Garofalo M, Di Leva G, Romano G, Nuovo G, Suh SS, Ngankeu A, Taccioli C, Pichiorri F, Alder H, Secchiero P, et al. (2009). miR-221&222 regulate TRAIL resistance and enhance tumorigenicity through PTEN and TIMP3 downregulation. *Cancer Cell* **16**, 498–509.

[36] Gabriely G, Wurdinger T, Kesari S, Esau CC, Burchard J, Linsley PS, and Krichevsky AM (2008). MicroRNA 21 promotes glioma invasion by targeting matrix metalloproteinase regulators. *Mol Cell Biol* **28**, 5369–5380.

[37] Koli K, Ryynanen MJ, and Keski-Oja J (2008). Latent TGF-beta binding proteins (LTBPs)-1 and -3 coordinate proliferation and osteogenic differentiation of human mesenchymal stem cells. *Bone* **43**, 679–688.

[38] Chandramouli A, Simundza J, Pinderhughes A, and Cowin P (2011). Choreographing metastasis to the tune of LTBP. *J Mammary Gland Biol Neoplasia* **16**, 67–80.

[39] van der Slot AJ, Zuurmond AM, Bardoel AF, Wijmenga C, Pruijs HE, Sillence DO, Brinckmann J, Abraham DJ, Black CM, Verzijl N, et al. (2003). Identification of PLOD2 as telopeptide lysyl hydroxylase, an important enzyme in fibrosis. *J Biol Chem* **278**, 40967–40972.

[40] Piper M, Barry G, Hawkins J, Mason S, Lindwall C, Little E, Sarkar A, Smith AG, Moldrich RX, Boyle GM, et al. (2010). NFIA controls telencephalic progenitor cell differentiation through repression of the Notch effector Hes1. *J Neurosci* **30**, 9127–9139.

[41] Starnes LM, Sorrentino A, Ferracin M, Negrini M, Pelosi E, Nervi C, and Peschle C (2010). A transcriptome-wide approach reveals the key contribution of NFI-A in promoting erythroid differentiation of human CD34(+) progenitors and CML cells. *Leukemia* **24**, 1220–1223.

[42] Song HR, Gonzalez-Gomez I, Suh GS, Commins DL, Sposto R, Gilles FH, Deneen B, and Erdreich-Epstein A (2010). Nuclear factor IA is expressed in astrocytomas and is associated with improved survival. *Neuro Oncol* **12**, 122–132.

[43] Tsunedomi R, Ogawa Y, Iizuka N, Sakamoto K, Tamesa T, Moribe T, and Oka M (2010). The assessment of methylated *BASP1* and *SRD5A2* levels in the detection of early hepatocellular carcinoma. *Int J Oncol* **36**, 205–212.

[44] Hartl M, Nist A, Khan MI, Valovka T, and Bister K (2009). Inhibition of Myc-induced cell transformation by brain acid-soluble protein 1 (BASP1). *Proc Natl Acad Sci USA* **106**, 5604–5609.

[45] Green LM, Wagner KJ, Campbell HA, Addison K, and Roberts SG (2009). Dynamic interaction between *WT1* and *BASP1* in transcriptional regulation during differentiation. *Nucleic Acids Res* **37**, 431–440.

[46] Soutar AK (2011). Unexpected roles for PCSK9 in lipid metabolism. *Curr Opin Lipidol* **22**, 192–196.

[47] Reiche J, Theilig F, Rafiqi FH, Carlo AS, Militz D, Mutig K, Todiras M, Christensen EI, Ellison DH, Bader M, et al. (2010). SORLA/SORL1 functionally interacts with SPAK to control renal activation of Na(+)-K(+)-Cl(−) cotransporter 2. *Mol Cell Biol* **30**, 3027–3037.

[48] Cizkova M, Cizeron-Clairac G, Vacher S, Susini A, Andrieu C, Lidereau R, and Bieche I (2010). Gene expression profiling reveals new aspects of *PIK3CA* mutation in ERα-positive breast cancer: major implication of the Wnt signaling pathway. *PLoS One* **5**, e15647.

| gene name | miR-191 sequence | | target sequence |
|---|---|---|---|
| AUTS2 | gucgacgaaaacccuAAGGCAAc | \|\|\|\|\|\|\| | ugugauauauagauuctgUUGACUa |
| TIMP3 | gucgACGAAAACCCUAAGGCAac | \|\| \|\|\| \|\|\|\|\|\| | uuuaUGAAUUUUAUAUUCCGUga |
| LTBP1 | gucGACGAAAACCCUA-AGGCAAc | \|\|\| \|\|\|\| \|\| \|\|\|\|\|\| | uguCUGAUUUU--AAUGUCCGUUc |
| PLOD2 | gucgaCGAAAACCCUAAGGCAAc | \|\| \|\| \|\|\|\|\|\| | guugaGCCUUGCUUCUUCCGUUu |
| LIMCH1 | gucgACGAAAACCCUAAGG-CAAc | \|\|:\|\| \|\| \|\|\|\| \|\|\| | acagUGUUUAUGUUUUUCCUGUUu |
| NFIA | gucgacgaaaacccuAAGGCAAc | \|\|\|\|\|\|\| | acuuugguaucuacuUUCCGUUu |
| BASP1 | gucGACG-AA--AACCCUAAGG-CAAc | \|\|\|\| \|\| \|\|\| :\|\|\|\| \|\|\| | aguCUGCGUUCAUUGCAGUUCCAGUUu |
| SORL1 | gucGACG-AAAACCCUAAGG-CAAc | :\|\|: \| \|\|\| \|\|\|\|\| \|\|\| | ggaUUGUAUCUUGACAUUCCUGUUg |
| PCSK9 | gucgacgaaaacccuAAGGCAAc | \|\|\|\|\|\|\| | caggcauggaacuuuUUCCGUUa |

**Figure W1.** miR-191 target sequence.